CHINESE OPTICS LETTERS
Vol. 20, No. 3 | March 2022

# Photonic lattice-like waveguides in glass directly written by femtosecond laser for on-chip mode conversion

Yuying Wang (王宇莹)[1,†], Lijing Zhong (钟理京)[2,†], Zhi Chen (陈 智)[2*], Dezhi Tan (谭德志)[2**], Zaijin Fang (方再金)[3], Yi Yang (杨 弈)[4], Shengzhi Sun (孙盛芝)[5], Lüyun Yang (杨旅云)[6], and Jianrong Qiu (邱建荣)[1,4]

[1] Ningbo Femto & Nano Laser Technology Co., Ltd., Ningbo 315000, China

[2] Zhejiang Lab, Hangzhou 311100, China

[3] Guangdong Provincial Key Laboratory of Optical Fiber Sensing and Communications, Institute of Photonics Technology, Jinan University, Guangzhou 511443, China

[4] State Key Laboratory of Modern Optical Instrumentation, College of Optical Science and Engineering, Zhejiang University, Hangzhou 310027, China

[5] Laboratory of Infrared Materials and Devices, The Research Institute of Advanced Technologies, Ningbo University, Ningbo 315211, China

[6] Wuhan National Laboratory for Optoelectronics, Huazhong University of Science and Technology, Wuhan 430074, China

*Corresponding author: zhichen@zhejianglab.edu.cn

**Corresponding author: wctdz@zju.edu.cn

Received October 29, 2021 | Accepted December 29, 2021 | Posted Online January 24, 2022

**We report on a conceptually new type of waveguide in glass by femtosecond laser direct writing, namely, photonic lattice-like waveguide (PLLW). The PLLW's core consists of well-distributed and densified tracks with a sub-micron size of 0.62 μm in width. Specifically, a PLLW inscribed as hexagonal-shape input with a ring-shape output side was implemented to converse Gaussian mode to doughnut-like mode, and high conversion efficiency was obtained with a low insertion loss of 1.65 dB at 976 nm. This work provides a new freedom for design and fabrication of the refractive index profile of waveguides with sub-micron resolution and broadens the functionalities and application scenarios of femtosecond laser direct-writing waveguides in future 3D integrated photonic systems.**

**Keywords:** femtosecond laser; glass material; laser direct-writing waveguide; light mode conversion.
**DOI:** 10.3788/COL202220.031406

## 1. Introduction

Femtosecond laser direct writing (FLDW) has shown great potential for manufacturing diverse components of complete on-chip integrated photonics, including light source, modulator, light computation, and detection[1–4]. In particular, FLDW has shown many more unique advantages for exploitation of three-dimensional (3D) integrated photonic devices[5], with respect to the conventional manufacturing strategy for photonic structures. However, there are still many possibilities for the FLDW improvement, from the development of new physical processes to new processing technologies, to meet the requirement for development of 3D photonic devices with high performance.

As is known, local modification triggered by nonlinear absorption of femtosecond pulses in a well-confined focal region is very complicated, including electronic excitation, relaxation, and thermal effect. Particularly, due to the influence of thermal diffusion or accumulation, the final size of the modified region is routinely quite large, and its morphology is usually non-regular/non-symmetrical[6]. Even worse, when using higher pulse energy for inscribing high contrast waveguide[7–9], the structural cracks and voids with negative refractive index change appear in areas accompanied by the waveguide core with positive refractive index change because of the extremely destructive micro-explosion confined in the laser focus. All of these phenomena make the morphology and refractive index distribution of the FLDW waveguide unpredictable and ultimately lead to difficulty in controlling the guiding mode characteristics, including mode size, intensity distribution, polarization state, and coupling between adjacent waveguide arrays. To harness these issues, a few strategies containing laser beam shaping[10], writing path design[11], and temperature gradient assisted FLDW[12] have been attempted in some glasses. However, these methods are still limited by the large size of the waveguide (a few to tens of microns in diameter) and relatively rough control of the spatial distribution of the waveguide refractive index. To date, a finer tailoring with sub-micron resolution seems impossible in previous FLDW structures.

Herein, we propose a new concept to create 3D waveguides in glass called the photonic lattice-like waveguide (PLLW).

Guiding is supported by total internal reflection, which is achieved by an effective refractive index difference between a central photonic lattice-like core region and the surrounding pristine glass, and does not rely on the photonic bandgap effect. Interestingly, the PLLW is based on a sub-micro-sized densified track arrays imposing a positive refractive index change of the waveguide's core, which is completely distinct from the cases in the past[13–19]. By well distributing the densified tracks at sub-micron resolution, the PLLW is supposed to generate arbitrary guiding modes, including mode conversion in a single waveguide with high conversion efficiency.

## 2. Design and Numerical Simulation

A PLLW created by tightly distributed tracks with a hexagonal-shape input and a ring-shape output [Fig. 1(a) and insert] is implemented by designing each writing path. The width and length size of a single track is designed at $0.7\,\mu m \times 1.2\,\mu m$, and two adjacent tracks are designed at 0.8 μm and 1.3 μm apart from the $Y$ and $Z$ directions, respectively. Thus, the width and length of the hexagon are 4 μm and 5.1 μm, which is similar to the core diameter (4 μm) of the 976 nm single-mode fiber used for coupling. At the output end, the tracks are evenly distributed along the ring, and the angle between two adjacent tracks remains unchanged. The tracks are inscribed by the FLDW method, and their trajectories are continuously and independently controlled by translating the 3D nano-translation platform. As a result, a hexagon-shaped PLLW at the input slowly converts into a ring-shape PLLW with a radius of 8 μm. The difference in the lattice structure results in a change

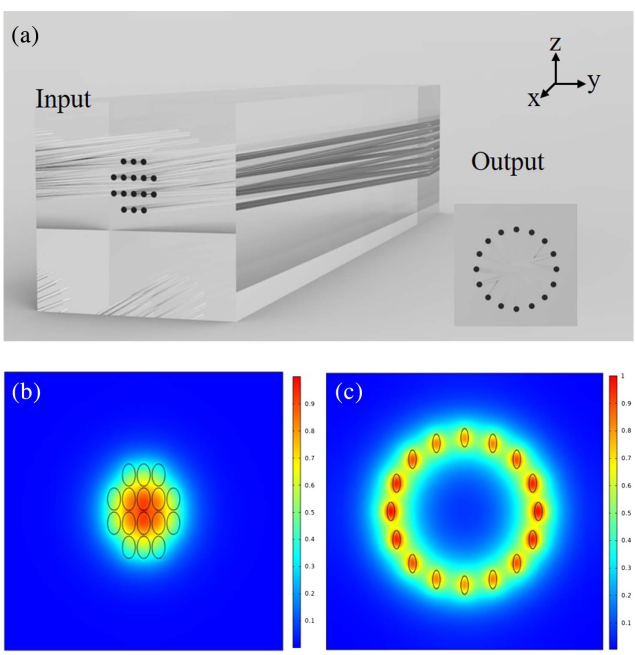


**Fig. 1.** Design scheme and simulation of PLLW. (a) Schematic diagram of PLLW. Insert: ring-shape output. (b) Simulated mode field of input side. (c) Simulated mode field of output side.

of the guiding mode. In principle, the PLLW can realize mode conversion between any two guiding modes by adjusting the writing path.

To understand the difference of guiding modes of PLLW at the input and output, a finite element method is used to study the mode fields of the photonic lattice structure. The refractive index difference between densified tracks and pristine material is set to $10^{-2}$[20]. The simulation results are shown in Figs. 1(b) and 1(c). The input mode field exhibits Gaussian-like distribution, while the output mode field shows doughnut-like distribution. It is notable that the field mode of the input and output is regulated within a few micrometers.

## 3. Femtosecond Laser Processing Experiments

To experimentally verify the feasibility of our theoretical design, a nanoporous silica glass (PG) with averaged pore size of ∼10 nm and porosity of ∼30% is used in this work[21–23]. Due to the characteristic structure of PG, superfluous pulse energy of the laser beam is dissipated out of the nanopores, and moderate densification is generated without residual lateral tensile or compressive stresses, so the FLDW tracks are proved to be stress-free in PG[24–26]. Thus, a tightly distributed waveguides array with quite low cross talk can effortlessly be fabricated in PG[27].

In our experiment, the tracks are fabricated with a chirped pulse amplified femtosecond Yb:KGd(WO$^4$)$^{20}$ (Yb:KGW) laser source (Pharos, Light Conversion) that delivers 226 fs pulses with 200 kHz repetition rate, and the central wavelength is 1030 nm. The scanning speed and depth of the FLDW tracks and PLLW are adjusted by a computer-controlled 3D nano-translation stage (SmartAct). The laser beam is linearly polarized and focused by a 100× microscope objective with a numerical aperture (NA) of 0.8. The laser pulse energy deposited on the PG is finely controlled by the continuous attenuator varying from 140 to 425 nJ. The pulse energy is measured after the attenuator, and about 60% of the pulse energy is deposited on the sample. The laser beam is focused vertically on the PG with the scanning speed of gradient change from 20 to 1000 μm/s.

The processing parameter window of the FLDW single track in the PG is shown in Fig. 2(a). Region I represents the partial densification tracks that can be inscribed at low pulse energy and/or high scanning speed, as shown in Fig. 2(b) (typical top view). In this region, the writing trace exhibits small positive refractive index change. The transition from partial densification to complete densification occurs in region II, and its typical example is shown in Fig. 2(c), where the tracks appear as a bright line, indicating a greater increase in refractive index compared to region I. As femtosecond laser pulse energy increases and/or the scanning speed decreases, due to enhanced energy accumulation in the modified region, voids appear in the center of damaged tracks with negative refractive index change [see typical top-view shown in Fig. 2(d)].

Since the refractive index change in region II is considerably positive, and no voids appear, region II is deliberately

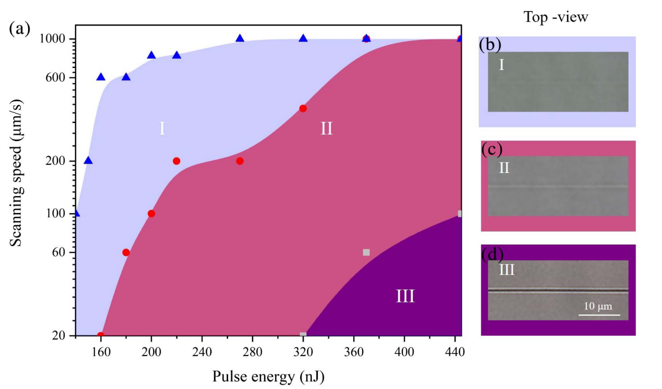


**Fig. 2.** (a) Processing parameter window of the FLDW single track in PG. Top-view of different regional tracks consistent with window (b) I, (c) II, and (d) III in (a), respectively. All of the tracks are written with depths of 200 μm.

distinguished and selected to process PLLW. The laser scanning speed of 40 μm/s is selected to verify the effect of direct-writing depths on the track size. With the increase of direct-writing depth, the pulse energy is gradually increased (from 55 to 185 nJ) to ensure that the refractive index changes of tracks are basically the same. As shown in Fig. 3, the length of tracks changes from 1.67 to 3.50 μm as the direct-writing depth increases from 10 to 200 μm due to influence of surface aberration. On the contrary, the width of the tracks is basically constant and less than 1 μm as the direct-writing depth increases, and the minimum width of densified track is 0.62 μm. By calculating the diffraction limit of the objective with NA = 0.8, the diffraction limits in the $Z$-axis direction and $XY$ direction are 3.22 μm and 0.66 μm, respectively. Notably, all of these densified tracks are below or comparable to the diffraction limit, which further indicates that the modified region by femtosecond laser is limited to a small area within the laser focus, owing to strong nonlinear absorption. However, due to the larger heat-affected zone, the modified region of femtosecond laser is larger than the laser focusing region in other glasses, and tracks are generally several microns[28]. Thus, we believe that such sub-micron-sized tracks can provide a new freedom for design and fabrication of PLLW in PG.

## 4. Results and Discussion

Based on the study on densification parameters of tracks and design scheme of PLLW, two waveguides are fabricated by FLDW in PG, namely, same hexagonal-shape input with width of 4 μm and ring-shape output with two different radii of 4 μm and 8 μm. In order to ensure good distribution of densified tracks and the same shape as the hexagon, the direct-writing depth is increased from 100 μm at the input to 170 μm at the output, and scanning speed is 40 μm/s.

The hexagonal-shape inputs of the two PLLWs have the same width and length of 4 μm, as shown in Figs. 4(a) and 4(c). Due to the influence of surface aberration, the ring becomes ellipse like, as shown in Figs. 4(b) and 4(d). The major and minor axes of the ellipse with the designed radii of 4 and 8 μm are measured as 8.1 μm × 9.4 μm [Fig. 4(b)] and 16.4 μm × 22.1 μm [Fig. 4(d)], respectively.

The demonstration of the PLLW for mode conversion is governed in terms of near-field distribution and insertion losses. A typical end-coupling system is employed with a 976 nm single-mode fiber laser (MChlight) with core diameter of 4 μm. The near-field intensity distribution is collected by a 50× microscope objective (NA = 0.55) and imaged by a CCD camera (ISH1000, TUCSEN). Moreover, the intensity curves of the input and output near-field distributions are recorded by a beam profiler (Photo, NanoScan 2). Figures 4(e) and 4(f) depict the measurement results of near-field distribution profiles, and

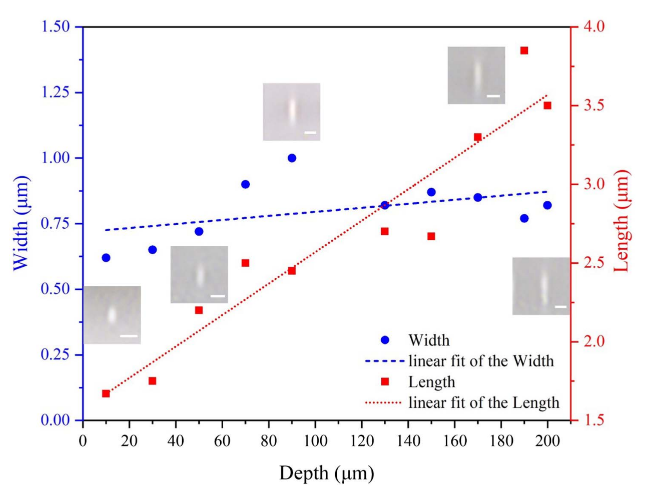


**Fig. 3.** Dependence of the width and length of densified tracks on FLDW depth. Inserts: microscopic cross-section images of tracks in different depths. Scale bar: 1 μm. All of the tracks are written with scanning speed of 40 μm/s in PG.

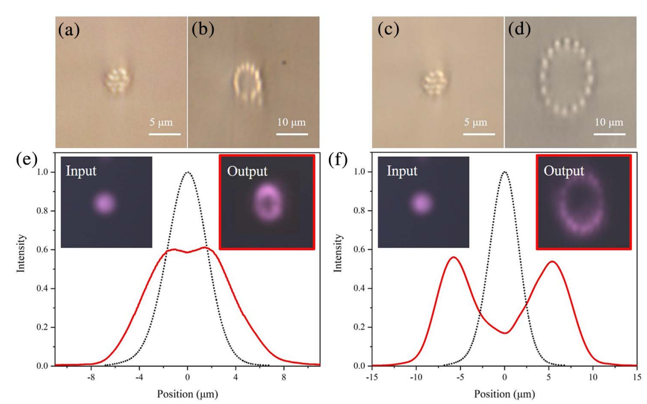


**Fig. 4.** Microscopic cross-section images of the PLLW (a) input and (b) output with a ring radius of 4 μm. The PLLW is written with scanning speed of 40 μm/s and pulse energy of 175 nJ. Microscopic cross-section images of the PLLW (c) input and (d) output with a ring radius of 8 μm. The PLLW is written with scanning speed of 40 μm/s and pulse energy of 165 nJ. The near-field distributions of PLLWs with a ring radius of (e) 4 μm and (f) 8 μm. Inserts: mode images of input and output sides.

the inserts show the measured mode images of the input and output sides. The full width at half-maximum (FWHM) of the input mode field is ~4.0 μm, which equals the core diameter of the 976 nm single-mode fiber used for coupling with the PLLW. All of the output mode fields of the two PLLWs show a doughnut-like distribution [Figs. 4(e) and 4(f)], characterized by a central intensity reduction of −4.9% and −71.4%, and the FWHM is 8.4 and 15.9 μm, respectively. The smallest radius of the doughnut-like mode is approximately 4.2 μm. Besides, the doughnut-like modes propagate stably in free space without changing their intensity distribution, so they are considered to be a superposition of the fundamental Gaussian mode and higher-order Laguerre–Gaussian modes[29]. Moreover, the reduction of central intensity means the decrease in the proportion of the fundamental Gussian mode[30]. Thus, a new degree of freedom for customizing the positive refractive index profile of FLDW waveguides at sub-micron resolution is demonstrated for on-chip mode conversion applications.

To evaluate the mode conversion efficiency, the insertion losses of the waveguide are estimated by measuring the input and output power directly. As the writing pulse energy changes from 115 to 185 nJ, the insertion losses measured increase from 1.65 and 3.20 dB. Fascinatingly, the insertion loss of 1.65 dB is quite low for FLDW waveguides in glass. The reason for such low insertion loss is that the hexagonal-shape input of the PLLW is centrosymmetric and nearly circular, which has been proved to have high coupling efficiency with the fiber used for coupling[10].

## 5. Conclusion

In conclusion, PLLW with a hexagonal-shape input and a ring-shape output is proposed, as a new concept of waveguide. The PLLW consists of 16 sub-micron sized densified tracks with positive refractive index change by FLDW in glass. The sub-micron tracks with minimum width of 0.62 μm have successfully been fabricated. Finally, a mode conversion application of PLLW with different shapes of input and output is demonstrated, which transforms the mode field from a Gaussian mode to a doughnut-like one with a high conversion efficiency indicated by the insertion loss as low as 1.65 dB at 976 nm, and its mode size can be controlled by tailoring the output ring shape. This work provides a new freedom for design and fabrication of waveguides with sub-micron resolution, which will contribute to development of on-chip all-optical integrated photonic devices in future.

## Acknowledgement

This work was supported by the National Key R&D Program of China (No. 2021YFB2800500), National Natural Science Foundation of China (Nos. U20A20211, 51902286, 61775192, 61905215, 51772270, 62105297, and 61905093), Zhejiang Provincial Natural Science Foundation (No. LQ22F050022), State Key Laboratory of High Field Laser Physics, Shanghai Institute of Optics and Fine Mechanics, Chinese Academy of Sciences, and Fundamental Research Funds for the Central Universities.

†These authors contributed equally to this work.

## References

1. G. Corrielli, A. Crespi, and R. Osellame, "Femtosecond laser micromachining for integrated quantum photonics," Nanophotonics **10**, 3789 (2021).
2. Y. Chen, J. Gao, Z. Jiao, K. Sun, W. Shen, L. Qiao, H. Tang, X. Lin, and X. Jin, "Mapping twisted light into and out of a photonic chip," Phys. Rev. Lett. **121**, 233602 (2018).
3. A. Seri, G. Corrielli, D. Lago-Rivera, A. Lenhard, H. de Riedmatten, R. Osellame, and M. Mazzera, "Laser-written integrated platform for quantum storage of heralded single photons," Optica **5**, 934 (2018).
4. F. Shen, X. Shu, K. Zhou, H. Jiang, H. Xia, K. Xie, and L. Zhang, "Compact vector twist sensor using a small period long period fiber grating inscribed with femtosecond laser," Chin. Opt. Lett. **19**, 090601 (2021).
5. A. El Hassan, F. K. Kunst, A. Moritz, G. Andler, E. J. Bergholtz, and M. Bourennane, "Corner states of light in photonic waveguides," Nat. Photonics **13**, 697 (2019).
6. D. Tan, B. Zhang, and J. Qiu, "Ultrafast laser direct writing in glass: thermal accumulation engineering and applications," Laser Photonics Rev. **15**, 2000455 (2021).
7. D. Tan, Z. Wang, B. Xu, and J. Qiu, "Photonic circuits written by femtosecond laser in glass: improved fabrication and recent progress in photonic devices," Adv. Photonics **3**, 024002 (2021).
8. S. M. Eaton, M. L. Ng, R. Osellame, and P. R. Herman, "High refractive index contrast in fused silica waveguides by tightly focused, high-repetition rate femtosecond laser," J. Non-Cryst. Solids. **357**, 2387 (2011).
9. F. Yu, L. Wang, Y. Chen, Q. Chen, Z. Tian, X. Ren, and H. Sun, "Polarization independent quantum devices with ultra-low birefringence glass waveguides," J. Lightwave Technol. **39**, 1451 (2021).
10. Z. Li, X. Li, F. Yu, Q. Chen, Z. Tian, and H. Sun, "Circular cross section waveguides processed by multi-foci-shaped femtosecond pulses," Opt. Lett. **46**, 520 (2021).
11. G. Corrielli, A. Crespi, R. Geremia, R. Ramponi, L. Sansoni, A. Santinelli, P. Mataloni, F. Sciarrino, and R. Osellame, "Rotated waveplates in integrated waveguide optics," Nat. Commun. **5**, 4249 (2014).
12. D. Tan, X. Sun, Q. Wang, P. Zhou, Y. Liao, and J. Qiu, "Fabricating low loss waveguides over a large depth in glass by temperature gradient assisted femtosecond laser writing," Opt. Lett. **45**, 3941 (2020).
13. Y. Jia, S. Wang, and F. Chen, "Femtosecond laser direct writing of flexibly configured waveguide geometries in optical crystals: fabrication and application," Opto-Electron. Adv. **3**, 190042 (2020).
14. G.-L. Roth, S. Kefer, S. Hessler, C. Esen, and R. Hellmann, "Polymer photonic crystal waveguides generated by femtosecond laser," Laser Photonics Rev. **15**, 2100215 (2021).
15. W. Nie, R. He, C. Cheng, U. Rocha, J. Rodriguez Vazquez de Aldana, D. Jaque, and F. Chen, "Optical lattice-like cladding waveguides by direct laser writing: fabrication, luminescence, and lasing," Opt. Lett. **41**, 2169 (2016).
16. Y. Jia, C. Cheng, J. R. Vázquez de Aldana, and F. Chen, "Three-dimensional waveguide splitters inscribed in Nd:YAG by femtosecond laser writing: realization and laser emission," J. Lightwave Technol. **34**, 1328 (2016).
17. G. R. Castillo, L. Labrador-Paez, F. Chen, S. Camacho-Lopez, and J. R. V. de Aldana, "Depressed-cladding 3-D waveguide arrays fabricated with femtosecond laser pulses," J. Lightwave Technol. **35**, 2520 (2017).
18. B. Zhang, L. Wang, and F. Chen, "Recent advances in femtosecond laser processing of $LiNbO_3$ crystals for photonic applications," Laser Photonics Rev. **14**, 1900407 (2020).
19. R. Li, L. Sun, Y. Cai, Y. Ren, H. Liu, M. D. Mackenzie, and A. K. Kar, "Near-infrared lasing and tunable upconversion from femtosecond laser inscribed Nd, Gd:$CaF_2$ waveguides," Chin. Opt. Lett. **19**, 081301 (2021).
20. L. Zhong, R. A. Zakoldaev, M. M. Sergeev, V. P. Veiko, and Z. Li, "Porous glass density tailoring by femtosecond laser pulses," Opt. Quant. Electron. **52**, 49 (2020).

21. Y. Chu, Y. Yang, L. Liao, Y. Liu, Y. Ma, X. Hu, Y. Wang, Y. Xing, J. Peng, H. Li, N. Dai, J. Li, and L. Yang, "3D nanoporous silica rods for extra-large-core high-power fiber lasers," ACS Photonics **5**, 4014 (2018).
22. L. Yang, N. Dai, Z. Liu, Z. Jiang, J. Peng, H. Li, J. Li, M. Yamashita, and T. Akai, "Tailoring of clusters of active ions in sintered nanoporous silica glass for white light luminescence," J. Mater. Chem. **21**, 6274 (2011).
23. Z. Liu, N. Dai, H. Luan, Y. Sheng, J. Peng, Z. Jiang, H. Li, L. Yang, and J. Li, "Enhanced green luminescence in Ce-Tb-Ca codoped sintered porous glass," Opt. Express **18**, 21138 (2010).
24. V. P. Veiko, S. I. Kudryashov, M. M. Sergeev, R. A. Zakoldaev, P. A. Danilov, A. A. Ionin, T. V. Antropova, and I. N. Anfimova, "Femtosecond laser-induced stress-free ultra-densification inside porous glass," Laser Phys. Lett. **13**, 055901 (2016).
25. T. E. Itina, R. A. Zakoldaev, M. M. Sergeev, H. Ma, S. I. Kudryashov, O. S. Medvedev, and V. P. Veiko, "Ultra-short laser-induced high aspect ratio densification in porous glass," Opt. Mater. Express **9**, 4379 (2019).
26. V. P. Veiko, R. A. Zakoldaev, M. M. Sergeev, P. A. Danilov, S. I. Kudryashov, G. K. Kostiuk, A. N. Sivers, A. A. Ionin, T. V. Antropova, and O. S. Medvedev, "Direct laser writing of barriers with controllable permeability in porous glass," Opt. Express **26**, 28150 (2018).
27. L. Zhong, R. A. Zakoldaev, M. M. Sergeev, and V. P. Veiko, "Fluorescent bulk waveguide sensor in porous glass: concept, fabrication, and testing," Nanomaterials **10**, 2169 (2020).
28. B. Sun, F. Morozko, P. S. Salter, S. Moser, Z. Pong, R. B. Patel, I. A. Walmsley, A. Hazan, N. Barré, A. Jesacher, J. Fells, A. Katiyi, A. Novitsky, A. Karabchevsky, and M. J. Booth, "On-chip beam rotators, polarizers and adiabatic mode converters through low-loss waveguides with variable cross-sections," arXiv:2112.02688 (2021).
29. H. Norman and H. Weber, *Laser Resonators and Beam Propagation: Fundamentals, Advanced Concepts and Applications* (Springer, 2005).
30. Y. Xiao, X. Tang, C. Wan, Y. Qin, H. Peng, C. Hu, and B. Qin, "Laguerre–Gaussian mode expansion for arbitrary optical fields using a subspace projection method," Opt. Lett. **44**, 1615 (2019).